

## Mitapivat, a pyruvate kinase activator, improves transfusion burden and reduces iron overload in $\beta$ -thalassemic mice

by Alessandro Mattè, Penelope A. Kosinski, Enrica Federti, Lenny Dang, Antonio Recchiuti, Roberta Russo, Angela Siciliano, Veronica Riccardi, Anne Janin, Matteo Mucci, Christophe Leboeuf, Achille Iolascon, Carlo Brugnara, and Lucia De Franceschi

*Received: December 20, 2022.*

*Accepted: February 7, 2023.*

*Citation: Alessandro Mattè, Penelope A. Kosinski, Enrica Federti, Lenny Dang, Antonio Recchiuti, Roberta Russo, Angela Siciliano, Veronica Riccardi, Anne Janin, Matteo Mucci, Christophe Leboeuf, Achille Iolascon, Carlo Brugnara, and Lucia De Franceschi. Mitapivat, a pyruvate kinase activator, improves transfusion burden and reduces iron overload in  $\beta$ -thalassemic mice.*

*Haematologica. 2023 Feb 16. doi: 10.3324/haematol.2022.282614 [Epub ahead of print]*

### *Publisher's Disclaimer.*

*E-publishing ahead of print is increasingly important for the rapid dissemination of science. Haematologica is, therefore, E-publishing PDF files of an early version of manuscripts that have completed a regular peer review and have been accepted for publication. E-publishing of this PDF file has been approved by the authors. After having E-published Ahead of Print, manuscripts will then undergo technical and English editing, typesetting, proof correction and be presented for the authors' final approval; the final version of the manuscript will then appear in a regular issue of the journal. All legal disclaimers that apply to the journal also pertain to this production process.*

## **Mitapivat, a pyruvate kinase activator, improves transfusion burden and reduces iron overload in $\beta$ -thalassemic mice**

Alessandro Mattè<sup>1</sup>, Penelope A. Kosinski<sup>2</sup>, Enrica Federti<sup>1</sup>, Lenny Dang<sup>2</sup>, Antonio Recchiuti<sup>3</sup>, Roberta Russo<sup>4</sup>, Angela Siciliano<sup>1</sup>, Veronica Riccardi<sup>1</sup>, Anne Janin<sup>5</sup>, Matteo Mucci<sup>3</sup>, Christophe Leboeuf<sup>5</sup>, Achille Iolascon<sup>4</sup>, Carlo Brugnara<sup>6</sup>, and Lucia De Franceschi<sup>1</sup>

<sup>1</sup> University of Verona and AOUI Verona, Verona, Italy;

<sup>2</sup> Agios Pharmaceuticals, Inc., Cambridge, MA, (USA);

<sup>3</sup> Dept. of Medical, Oral and Biotechnology Science, "G. d'Annunzio" University of Chieti, Chieti, Italy;

<sup>4</sup> Dept. of Molecular Medicine and Medical Biotechnology and CEINGE, University of Naples Federico II, Naples, Italy;

<sup>5</sup> University Diderot of Paris, Paris, France;

<sup>6</sup> Department of Laboratory Medicine, Harvard Medical School, Boston Children's Hospital, Boston, MA (USA).

Running title: Mitapivat in chronic transfused beta thal mice

Key words:  $\beta$ -thalassemia, kidney fibrosis, transfusion burden, miRNA

Words count: 1348.

### Corresponding author:

Lucia De Franceschi, MD

Dept of Medicine, University of Verona & AOUI Verona, Verona, Italy;

Phone: +390458128419;

Fax: +390458027473;

e-mail: [lucia.defranceschi@univr.it](mailto:lucia.defranceschi@univr.it)

### **AUTHOR CONTRIBUTIONS**

LDF, CB, AM, AI designed and carried out research and wrote the paper. PAK, LD, CB critically revised data and wrote the paper. AM, EF, AS, VR carried out cytokine

FACS analysis, immunoprecipitation assays, and ELISA analysis. RB carried out molecular analysis. EF revised the paper. MM, AR carried out miRNA analysis, analyzed the data, and wrote the paper. CL, AJ performed pathology, analyzed data.

### **ACKNOWLEDGEMENTS**

This study was supported by an Agios Pharmaceuticals, Inc. research collaborative grant to LDF. Editorial assistance was provided by Avant Healthcare, LLC and Excel Medical Affairs, Horsham, UK, supported by Agios.

### **AUTHORS DISCLOSURES**

LDF has received research funding from Agios during 2015-2022. LD and PAK are Agios employees and stockholders.

### **DATA-SHARING STATEMENT**

All the data and protocols are stored in the Nas Synology DS216se Hard Disk, located at the University of Verona, 37134 Verona, Italy and will be available on request.

Please direct requests for original data to the corresponding author email:

[lucia.defranceschi@univr.it](mailto:lucia.defranceschi@univr.it)

### **ETHICS STATEMENT**

Ethics statement about the treatment of the laboratory mice: The Institutional Animal Experimental Committee of University of Verona (CIRSAL) and the Italian Ministry of Health approved the experimental protocols (56DC9.64), following European directive 2010/63/EU and the Federation for Laboratory Animal Science Associations guidelines and recommendations.

## To the Editor:

$\beta$  thalassemia is a genetic red cell disorder characterized by chronic hemolytic anemia due to ineffective erythropoiesis and reduced red cell survival (1-3). Chronic transfusion and intensive iron chelation are standard treatments for  $\beta$  thalassemic syndromes (1), but new therapeutic options are being developed, including gene therapy (4) and novel pharmacologic approaches. We have shown that mitapivat, a pyruvate kinase activator, improves anemia and ineffective erythropoiesis in  $Hbb^{th3/+}$  mice, a widely used model for  $\beta$  thalassemia (5). The effects of mitapivat are not limited to the erythroid compartment: mitapivat also modulates DMT1 expression, controlling iron absorption in the duodenum in  $Hbb^{th3/+}$  mice, with an increase of hepcidin related to the improvement in ineffective  $\beta$ -thalassemic erythropoiesis (5). Results from a phase 2 trial of mitapivat in non-transfusion-dependent thalassemic (NTDT) patients previously demonstrated a sustained long-term increase in hemoglobin (Hb  $\geq 1$  g/dL) with improvement of hemolysis and ineffective erythropoiesis (6). Here, we asked whether mitapivat might be a potential therapeutic option also for  $\beta$ -thal patients under chronic transfusion regimen. To address this question, we exposed female  $Hbb^{th3/+}$  mice (3-4 months of age) to chronic transfusion with or without mitapivat (50 mg/Kg twice daily) treatment.  $Hbb^{th3/+}$  mice were treated by oral gavage with mitapivat (50 mg/Kg BID) or vehicle for 10 days, and then transfused with 400  $\mu$ L washed red cells at 40-45% Hematocrit (Hct) (7) (Figure 1a). We defined Hb values  $\leq 10.5$  g/dL as transfusion threshold, corresponding to the reduction of  $\sim 50\%$  of post-transfusion Hb values. Normality of data was assessed with the Shapiro-Wilk test. Two-tailed unpaired Student t-test or two-way analysis of variance with Tukey's multiple comparisons were used for data analyses. Data show values from individual mice and are presented with mean  $\pm$  SEM (differences with  $P < 0.05$  were considered significant). As shown in Figure 1b, Mitapivat-treated  $\beta$ -thal mice exposed to chronic transfusion displayed a greater sustained rise in Hb from baseline compared to vehicle-treated transfused  $\beta$ -thal mice. This resulted in a longer interval between transfusions ( $13.8 \pm 1.0$  days in mitapivat-treated  $\beta$ -thal mice vs  $10.5 \pm 1.0$  days in vehicle-treated  $\beta$ -thal mice, Figure 1c). Chronic transfusion resulted in a significant reduction of splenomegaly in both mitapivat- and vehicle-treated  $\beta$ -thal mice (Figure 1Sa) compared to untreated  $\beta$ -thal mice, but spleen iron accumulation was significantly

lower in mitapivat-treated  $\beta$ -thal mice when compared to vehicle-treated  $\beta$ -thal mice (Figure 1d). A significant reduction of both bone marrow and spleen ineffective erythropoiesis was observed in all transfused  $\beta$ -thal mice (Figure 1e, Figure 1Sb). Of note, mitapivat-treated transfused  $\beta$ -thal mice showed a slight increase of bone marrow erythropoiesis with a trend towards an improvement of maturation index compared to vehicle-treated transfused  $\beta$ -thal mice evaluated at the end of the study (5). This is most likely related to a protective effect of mitapivat on residual bone marrow and spleen erythropoiesis (Figure 1f). Indeed, plasma erythropoietin was lower in mitapivat-treated transfused  $\beta$ -thal mice than in vehicle-treated transfused  $\beta$ -thal mice (Figure 1Sc). Since splenic macrophages contribute to both erythrophagocytosis and iron recycling, we evaluated the functional profile of spleen macrophages in the different mouse groups (8). As shown in Figure 1g, flow cytometric analysis of the surface expression of the M1 marker CD80 and the M2 marker CD206 on spleen macrophages ( $M\Phi$ ) revealed that mitapivat promoted a pro-resolving profile of splenic macrophages in transfused  $\beta$ -thal mice when compared to vehicle-treated transfused  $\beta$ -thal mice (Figure 2Sa). This effect was still observed in non-transfused mitapivat-treated mice compared to vehicle-treated  $\beta$ -thal mice (Figure 1g, 2Sa). Collectively, these data support the role of mitapivat in reprogramming macrophages from pro-inflammatory to pro-resolving and repairing the phenotype in  $\beta$ -thal mice with or without chronic transfusion (9).

We then evaluated the impact of mitapivat on iron metabolism in transfused  $\beta$ -thal mice. Mitapivat-treated transfused  $\beta$ -thal mice showed lower liver iron accumulation when compared to vehicle-treated transfused  $\beta$ -thal mice (Figure 2a). This might be due in part to the reduction of the transfusion burden but also to the multimodal action of mitapivat, which we previously showed to modulate hepcidin indirectly by the reduction of ineffective erythropoiesis and downregulation of DMT1 expression in the duodenum (5). Indeed, in mitapivat-treated transfused  $\beta$ -thal, we found a significant increase in liver hepcidin/LIC ratio (Figure 2b) and a marked reduction in the percentage of serum transferrin saturation when compared to vehicle-treated transfused  $\beta$ -thal mice (Figure 2c). The reduced transfusion burden observed in mitapivat treated  $\beta$ -thal mice might favorably contribute to the general reduction of iron-overload in  $\beta$ -thal mice exposed to chronic transfusion. Our pre-clinical results in combination with clinical data from NTDT patients treated with

mitapivat (6) suggest that the increase in the length of time between transfusions with mitapivat treatment may be associated with improvement in the quality of life in patients as well as a decrease in iron-overload-related organ damage.

Recent reports in TDT patients have highlighted a correlation between ferritin levels and kidney iron accumulation assessed by magnetic resonance T2\* imaging, or in sample analysis from kidney biopsies or autopsy series (10). Kidney iron overload mainly involved the tubular compartment which has been related to chronic anemia and might be reversed by iron chelation (10). In vehicle-treated transfused  $\beta$ -thal mice, we found tubular accumulation of iron, which was significantly reduced in mitapivat-treated transfused animals (Figure 3a). No major difference in creatinine was observed in both  $\beta$ -thal mouse groups exposed to chronic transfusion (Figure 2Sb). Previous studies suggest that kidney iron accumulation promotes local oxidative stress, contributing to profibrotic signaling in addition to hypoxia (10, 11). miRNA let-7b, -c, and -d have been shown to be linked to renal fibrosis throughout the transforming growth factor- $\beta$  cascade (TGF- $\beta$ ) (12). In this study, miRNA let-7b and -d were upregulated in vehicle-treated  $\beta$ -thal mice with or without chronic transfusion (Figure 3b, 2Sc), while mitapivat downregulated miRNA let-7b and -d in  $\beta$ -thal mice with or without chronic transfusion (Figure 3b, 2Sc).

miRNAs let-7 have been reported to reduce ATP production by deactivating pyruvate dehydrogenase kinase (PDK) (13). Here, we found normalization of the amount of the active form of the TGF- $\beta$  receptor in  $\beta$ -thal mice treated with mitapivat when compared to vehicle-treated  $\beta$ -thal mice with or without transfusion (Figure 3c). Previously, in  $\beta$ -thal mice, the activation of TGF- $\beta$  receptor was reduced by chronic transfusion, hypoxia being a trigger of activation of TGF- $\beta$  receptor (14). Taken together, our data indicate that mitapivat might play a pivotal role in kidney protection by reducing the transfusion burden and iron overload as well as by preserving energy cell metabolism. This might represent an added value of mitapivat as a therapeutic option for patients with  $\beta$ -thal taking iron chelators who develop renal toxicity or chronic kidney disease.

Finally, we explored the effects of the coadministration of mitapivat and deferiprone (DFP) on  $\beta$ -thal mice, since iron chelation is part of the gold standard treatment of TDT patients (1). DFP was administered to Hbb<sup>th3/+</sup> mice treated with mitapivat in drinking water at the dosage of either 1.25 or 0.75 mg/ml (15) (Figure

3Sa). Previously, Casu et al reported that DFP alone has no effect on hematologic parameters and red cell features in murine  $\beta$ -thal (15). The beneficial effects of mitapivat on murine  $\beta$ -thal anemia was maintained when mitapivat was co-administered with DFP at both dosages, as supported by the stable and sustained increase in Hb and the reduction in circulating erythroblasts compared to baseline values (Figure 3Sb, c). In agreement with Matte et al.(5), we found a significant reduction in  $\alpha$ -globin membrane precipitates in red cells from mitapivat-DFP treated Hbb<sup>th3/+</sup> mice compared with vehicle-treated animals (Figure 3Sd). Of note, DFP iron chelation efficacy represented by a change in LIC was preserved in  $\beta$ -thal mice treated with both DFP and mitapivat (Figure 3Se).

In conclusion, our study shows for the first time that mitapivat improves the transfusion burden and reduces organ iron overload in  $\beta$ -thal mice exposed to a chronic transfusion regimen. We also observed that mitapivat might protect the kidney against profibrotic stimuli related to local iron accumulation by two different mechanisms: the reduction in transfusion requirement and the local modulation of miRNA involved in profibrotic signaling. Finally, the observed reprogramming of spleen macrophages toward a pro-resolving phenotype might represent an added value to the known improvement of ineffective erythropoiesis induced by mitapivat in  $\beta$ -thal mice (5). Thus, the beneficial effects of mitapivat in  $\beta$ -thal mice exposed to chronic transfusion support its use as a potential new therapeutic tool in clinical management of thalassemic patients under chronic transfusion regimen.

## **REFERENCES**

1. Taher AT, Musallam KM, Cappellini MD. beta-Thalassemias. *N Engl J Med*. 2021;384(8):727-743.
2. De Franceschi L, Bertoldi M, Matte A, et al. Oxidative stress and  $\beta$ -thalassemic erythroid cells behind the molecular defect. *Oxid Med Cell Longev*. 2013;2013:985210.
3. Rivella S.  $\beta$ -thalassemias: paradigmatic diseases for scientific discoveries and development of innovative therapies. *Haematologica*. 2015;100(4):418-430.
4. Locatelli F, Thompson AA, Kwiatkowski JL, et al. Betibeglogene Autotemcel Gene Therapy for Non-beta(0)/beta(0) Genotype beta-Thalassemia. *N Engl J Med*. 2022;386(5):415-427.
5. Matte A, Federti E, Kung C, et al. The pyruvate kinase activator mitapivat reduces hemolysis and improves anemia in a beta-thalassemia mouse model. *J Clin Invest*. 2021;131(10):e144206.
6. Kuo KHM, Layton DM, Lal A, et al. Safety and efficacy of mitapivat, an oral pyruvate kinase activator, in adults with non-transfusion dependent alpha-thalassaemia or beta-thalassaemia: an open-label, multicentre, phase 2 study. *Lancet*. 2022;400(10351):493-501.
7. Park SY, Matte A, Jung Y, et al. Pathologic angiogenesis in the bone marrow of humanized sickle cell mice is reversed by blood transfusion. *Blood*. 2020;135(23):2071-2084.
8. Ramos P, Casu C, Gardenghi S, et al. Macrophages support pathological erythropoiesis in polycythemia vera and beta-thalassemia. *Nat Med*. 2013;19(4):437-445.
9. Galvan-Pena S, O'Neill LA. Metabolic reprogramming in macrophage polarization. *Front Immunol*. 2014;5:420.
10. Demosthenous C, Vlachaki E, Apostolou C, et al. Beta-thalassemia: renal complications and mechanisms: a narrative review. *Hematology*. 2019;24(1):426-438.
11. Musallam KM, Taher AT. Mechanisms of renal disease in beta-thalassemia. *J Am Soc Nephrol*. 2012;23(8):1299-1302.
12. Hong S, Lu Y. Omega-3 fatty acid-derived resolvins and protectins in inflammation resolution and leukocyte functions: targeting novel lipid mediator pathways in mitigation of acute kidney injury. *Front Immunol*. 2013;4:13.
13. Ma X, Li C, Sun L, et al. Lin28/let-7 axis regulates aerobic glycolysis and cancer progression via PDK1. *Nat Commun*. 2014;5:5212.
14. Chou YH, Pan SY, Shao YH, et al. Methylation in pericytes after acute injury promotes chronic kidney disease. *J Clin Invest*. 2020;130(9):4845-4857.
15. Casu C, Aghajan M, Oikonomidou PR, et al. Combination of Tmprss6- ASO and the iron chelator deferiprone improves erythropoiesis and reduces iron overload in a mouse model of beta-thalassemia intermedia. *Haematologica*. 2016;101(1):e8-e11.

## **FIGURE LEGENDS**

### **Figure 1. Mitapivat reduces transfusion burden in $\beta$ -thal mice exposed to chronic transfusion with associated reprogramming of splenic macrophage phenotype.**

- a.** Experimental study design to assess the effects of mitapivat on hematologic phenotype of  $\beta$ -thal mice exposed to chronic transfusion.
- b.** Hb changes over time in transfused (Tr.)  $\beta$ -thal ( $Hbb^{th3/+}$ ) mice treated with either vehicle or mitapivat (50 mg/Kg BID) shown as single animals (n=3 vehicle-treated mice; n=4 mitapivat-treated mice). Grey dotted line shows the transfusion threshold (10.5 g/dL).
- c.** Transfusion time intervals in  $\beta$ -thal ( $Hbb^{th3/+}$ ) mice treated with either vehicle or mitapivat (50 mg/Kg BID). Data are presented as means  $\pm$  SEM (n=3 vehicle-treated mice; n=4 mitapivat-treated mice);  $^{\#}P < 0.05$  compared to vehicle-treated transfused  $\beta$ -thal mice.
- d.** Iron staining (Perl's Prussian blue is a semi-quantitative method to assess organ iron accumulation) in spleen from  $Hbb^{th3/+}$  mice treated with either vehicle or transfusion plus vehicle or transfusion *plus* mitapivat. One representative image from 3 with similar results. **Left panel.** Quantification of iron staining in spleen. Data are mean  $\pm$  SEM (n=3).  $^*P < 0.05$  compared with vehicle  $Hbb^{th3/+}$  mice and  $^{\#}P < 0.05$  compared with vehicle-treated transfused  $Hbb^{th3/+}$  mice.
- e.** Flow cytometric analysis ( $CD44^{+}Ter119^{+}$  and cell size markers, see also Figure 2S) of bone marrow and spleen from  $Hbb^{th3/+}$  mice exposed to either vehicle or to chronic transfusion with and without mitapivat treatment (see also Matte et al. JCI 2021, (5)). Data are mean  $\pm$  SEM (n=3-4).  $^*P < 0.05$  compared with vehicle  $Hbb^{th3/+}$  mice and  $^{\#}P < 0.05$  compared with vehicle-treated transfused  $Hbb^{th3/+}$  mice.
- f.** Maturation index as ratio between pop II (Baso E.) and pop IV (Ortho E.) in bone marrow and spleen from  $Hbb^{th3/+}$  mice treated with either vehicle or exposed to chronic transfusion with or without mitapivat, analyzed by flow cytometry. Data are mean  $\pm$  SEM (n=3-4).
- g.** Flow cytometric quantification of M1 (CD80) and M2 (CD206) expression on spleen macrophage cell surface from wild type (WT) or  $Hbb^{th3/+}$  mice exposed to either vehicle or mitapivat or to chronic transfusion with and without mitapivat

treatment. Spleen M $\Phi$  were isolated with the GentleMACS cell dissociator (Miltenyi Biotech, Germany). M $\Phi$  were identified and gated as CD45<sup>+</sup>/F4/80<sup>+</sup> cells. Anti-CD45 PE-Cy5.5, F4/80 PE, CD206 PerCP-Cy5.5 and CD80 were from BioLegend, USA. Data are mean  $\pm$  SEM (n=3-4). MFI, mean fluorescence intensity.

**Figure 2. Mitapivat-treated transfused  $\beta$ -thal mice show reduced liver iron accumulation and improved iron homeostasis.**

**a. Left panel.** Iron staining (Perl's Prussian blue is a semi-quantitative method to assess organ iron accumulation) in liver from wild type (WT) and Hbb<sup>th3/+</sup> mice treated with either vehicle or transfusion or transfusion *plus* mitapivat. One representative image from 5 with similar results. **Right panel.** Quantification of iron staining in liver. Data are mean  $\pm$  SEM (n=5). <sup>o</sup>  $P < 0.05$  compared to wild-type, \* $P < 0.05$  compared with vehicle Hbb<sup>th3/+</sup> mice and # $P < 0.05$  compared with vehicle-treated transfused Hbb<sup>th3/+</sup> mice.

**b.** Liver mRNA expression normalized over liver iron concentration (LIC) as determined using the bathophenanthroline method. Data are presented as means  $\pm$  SEM (n=3). # $P < 0.05$  compared with vehicle-treated transfused Hbb<sup>th3/+</sup> mice.

**c.** Transferrin saturation in Hbb<sup>th3/+</sup> mice treated with either vehicle or transfusion or transfusion *plus* mitapivat. Transferrin saturation was calculated as the ratio between serum iron and total iron binding capacity, using the Total Iron Binding Capacity Kit (Randox Laboratories, UK) and 50  $\mu$ L of serum, according to the manufacturer's instructions. Data are presented as means  $\pm$  SEM (n=3). \* $P < 0.05$  compared with vehicle Hbb<sup>th3/+</sup> mice and # $P < 0.05$  compared with vehicle-treated transfused Hbb<sup>th3/+</sup> mice.

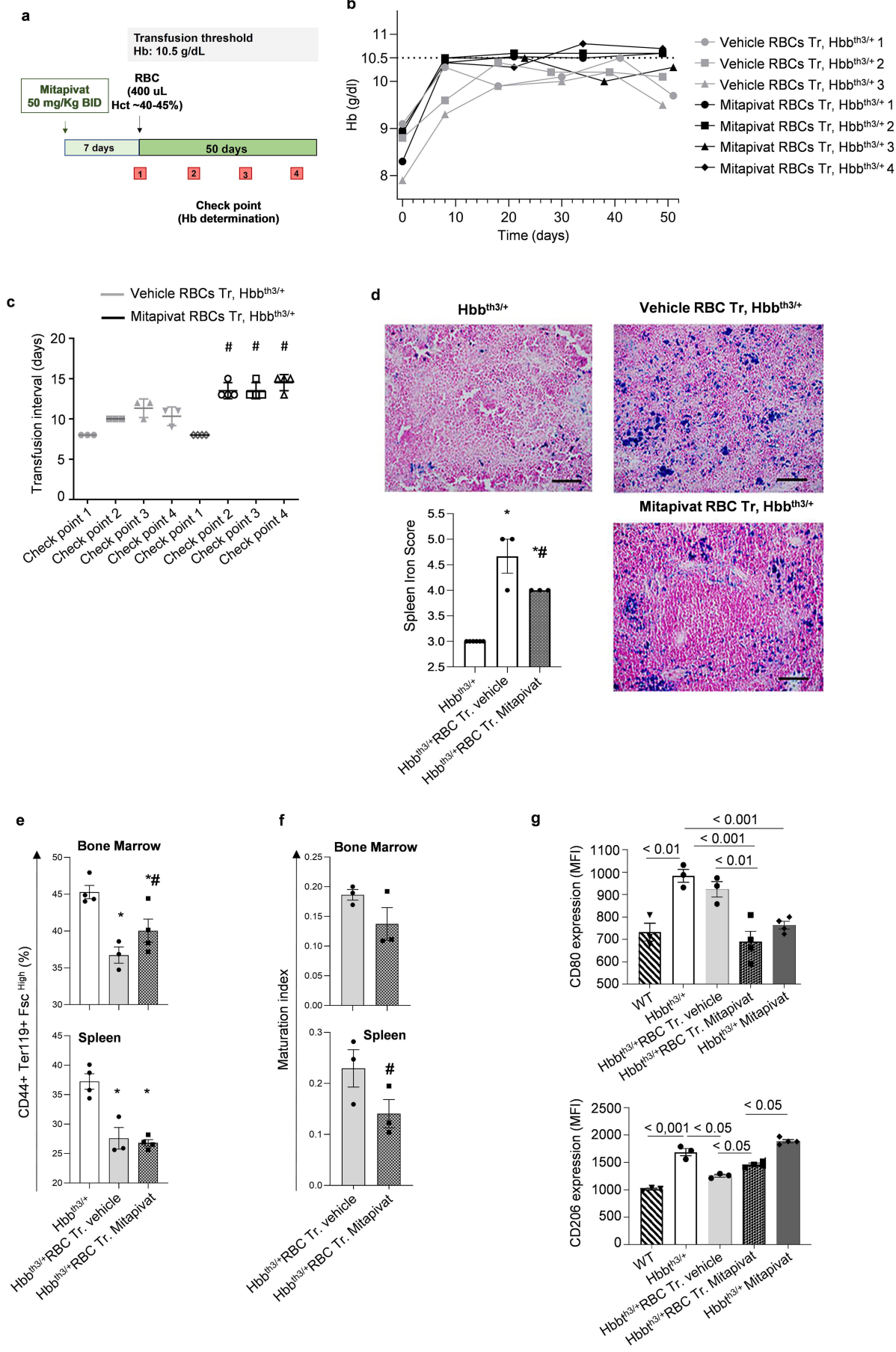
**Figure 3. In transfused  $\beta$ -thal mice, mitapivat reduces kidney iron accumulation and downregulates profibrotic kidney miRNA let-7 expression.**

**a. Upper panel.** Iron staining (Perl's Prussian blue is a semi-quantitative method to assess organ iron accumulation) in kidney from wild type (WT) and Hbb<sup>th3/+</sup> mice treated with either vehicle or transfusion or transfusion *plus* mitapivat. One representative image from 3-6 with similar results. **Lower panel.** Quantification of iron staining in kidney. Data are mean  $\pm$  SEM (n=3-6). \* $P < 0.05$  compared with

vehicle Hbb<sup>th3/+</sup> mice and #*P* < 0.05 compared with vehicle-treated transfused Hbb<sup>th3/+</sup> mice.

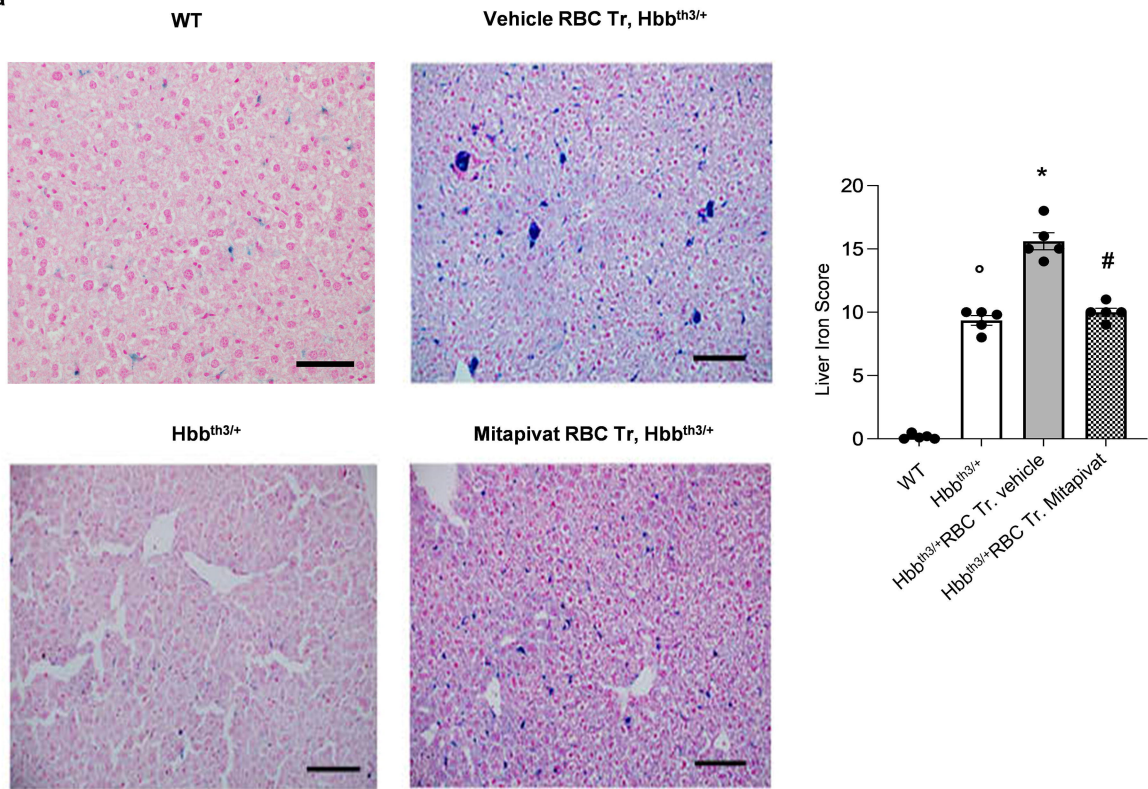
**b.** Relative expression of miRNAs let-7b and -7d in kidneys from wild type (WT) or Hbb<sup>th3/+</sup> mice exposed to either vehicle or mitapivat or to chronic transfusion with and without mitapivat treatment. Small RNA was isolated from frozen kidneys using a silica spin column-based Quick-RNA kit (Zymo Research), quantified with a UV NanoPhotometer (Implen), and reverse transcribed with the qScript microRNA cDNA Synthesis for RT-PCR (QuantaBio). For real time PCR analysis of let-7b and let-7d miRNAs, 3 ng of cDNA were used as a template in reaction mixtures (10 µL final volume) including a PowerUp SYBR Green Master Mix (5 µL, Applied Biosystems), miRNA-specific forward and universal reverse primers (1 µL each, miRCURY assays, Qiagen), and PCR-grade water. The expression of the indicated mRNAs was quantitated by the comparative  $\Delta$ Ct method. RNU6-1 was used as control for normalization. Data are mean  $\pm$  SEM (n=3-4). \**P* < 0.05. \*\* *P* < 0.01. \*\*\* *P* < 0.001.

**c.** Phospho-tyrosine immunoprecipitation of kidneys from wild type (WT) or Hbb<sup>th3/+</sup> mice exposed to either vehicle or mitapivat or to chronic transfusion with and without mitapivat treatment, using anti-phospho-tyrosine specific antibodies (IP: PY, clone PY99 from SCBT, Santa Cruz, CA and clone 4G10 from Merck KGaA, Darmstadt, Germany), revealed with anti-TGF- $\beta$  receptor (Rec) specific antibody. GAPDH in whole-cell lysate (WCL) is used as loading control. One representative gel from 4 others with similar results is presented. Blots were developed using the Luminata Forte Chemiluminescent HRP Substrate from Merck Millipore (Armstadt, Germany), and images were acquired with the Alliance Q9 Advanced imaging system (Uvitec, UK). Densitometric analysis of immunoblots is shown on the right. Data are mean  $\pm$  SEM (n=4). °*P* < 0.05 compared to wild-type; \**P* < 0.05 compared with vehicle Hbb<sup>th3/+</sup> mice, #*P* < 0.05 compared with vehicle-treated transfused Hbb<sup>th3/+</sup> mice.

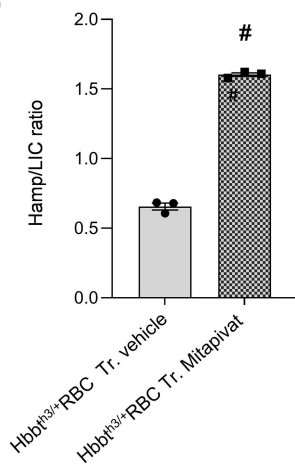
**Figure 1**

**Figure 2**

**a**



**b**



**c**

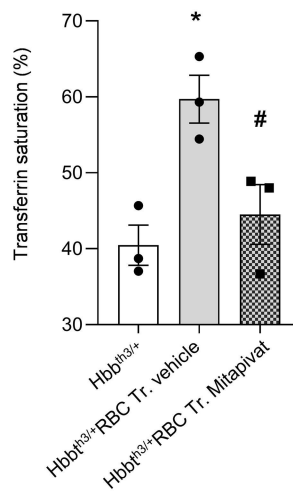
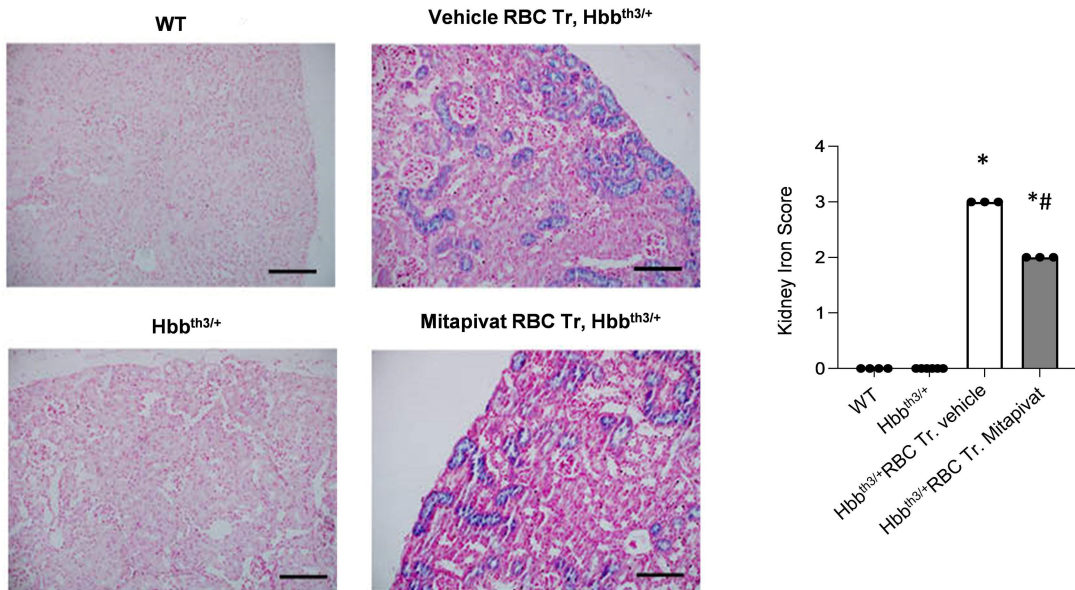
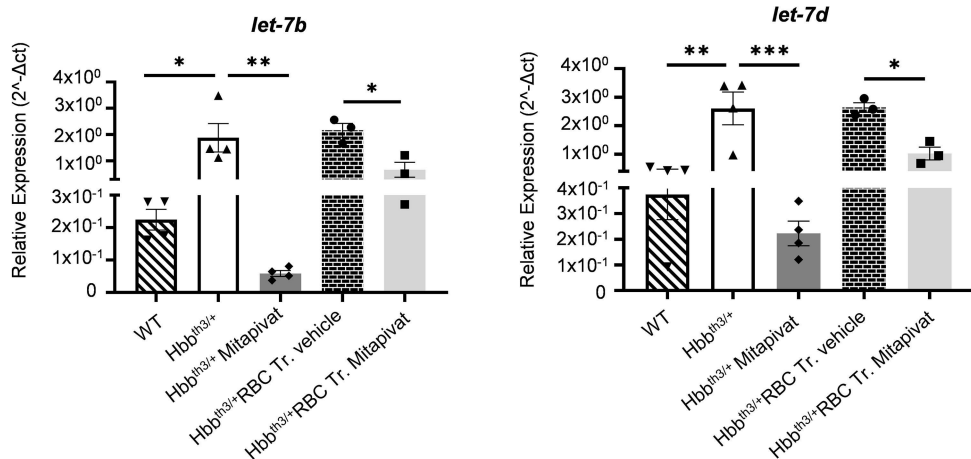


**Figure 3**

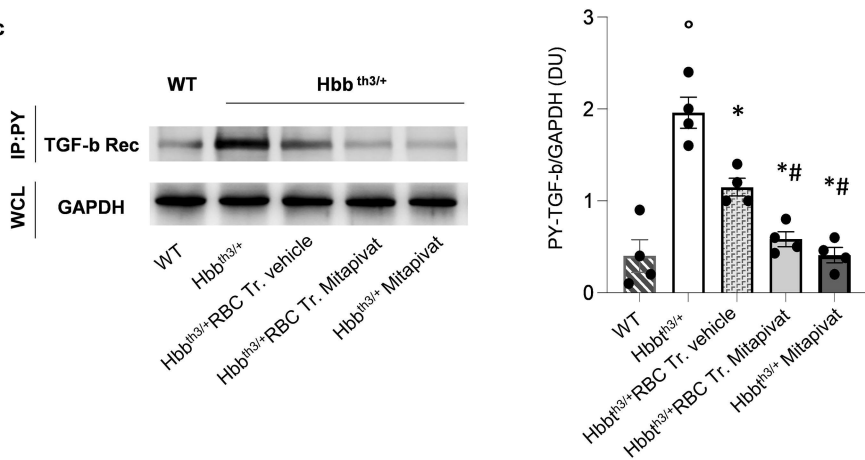
**a**



**b**

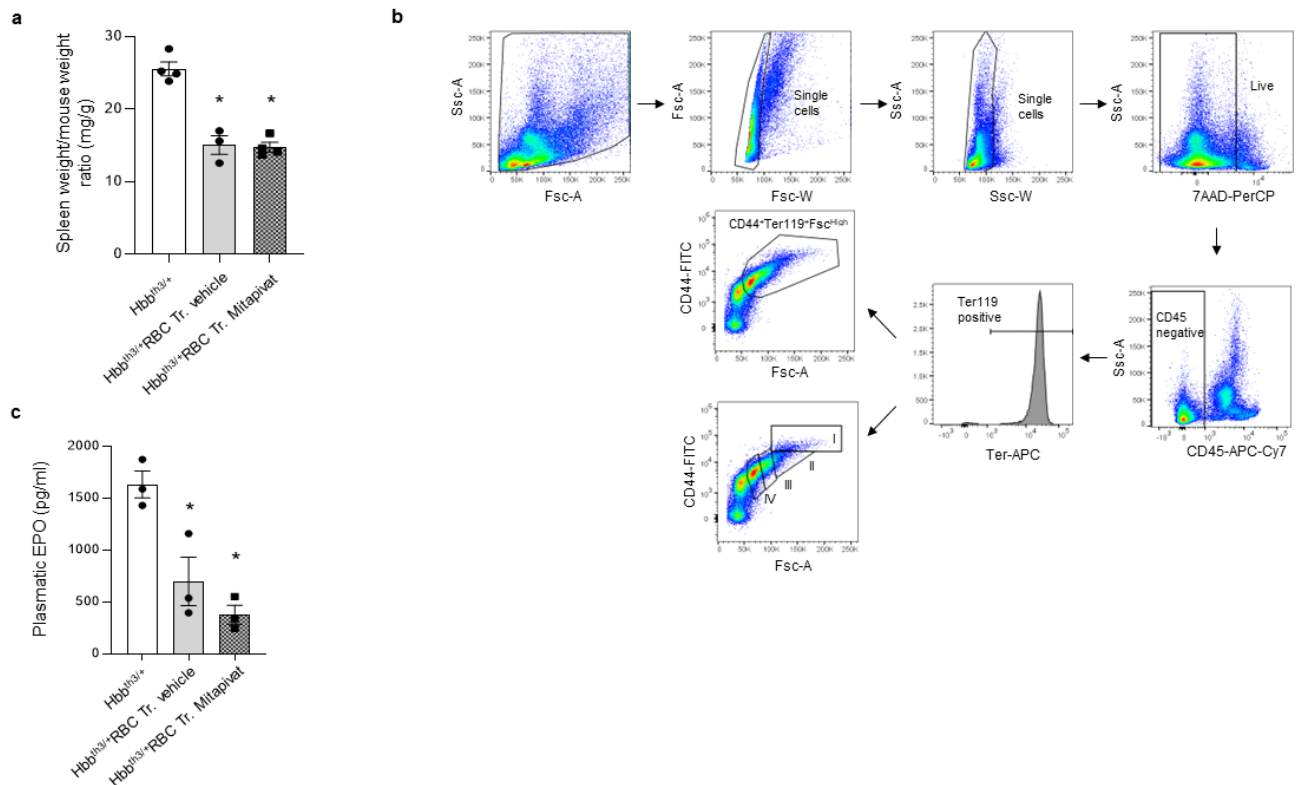


**c**



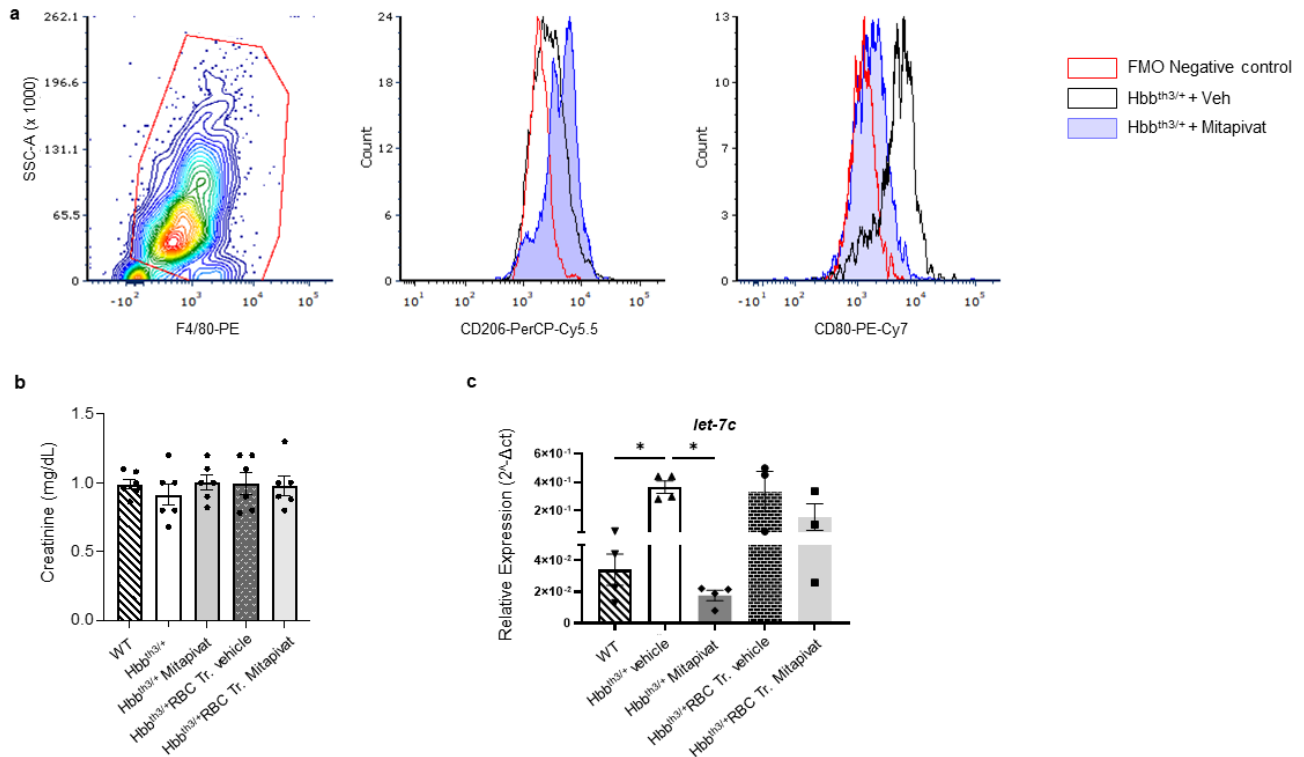
## SUPPLEMENTARY FIGURES

Figure 1S



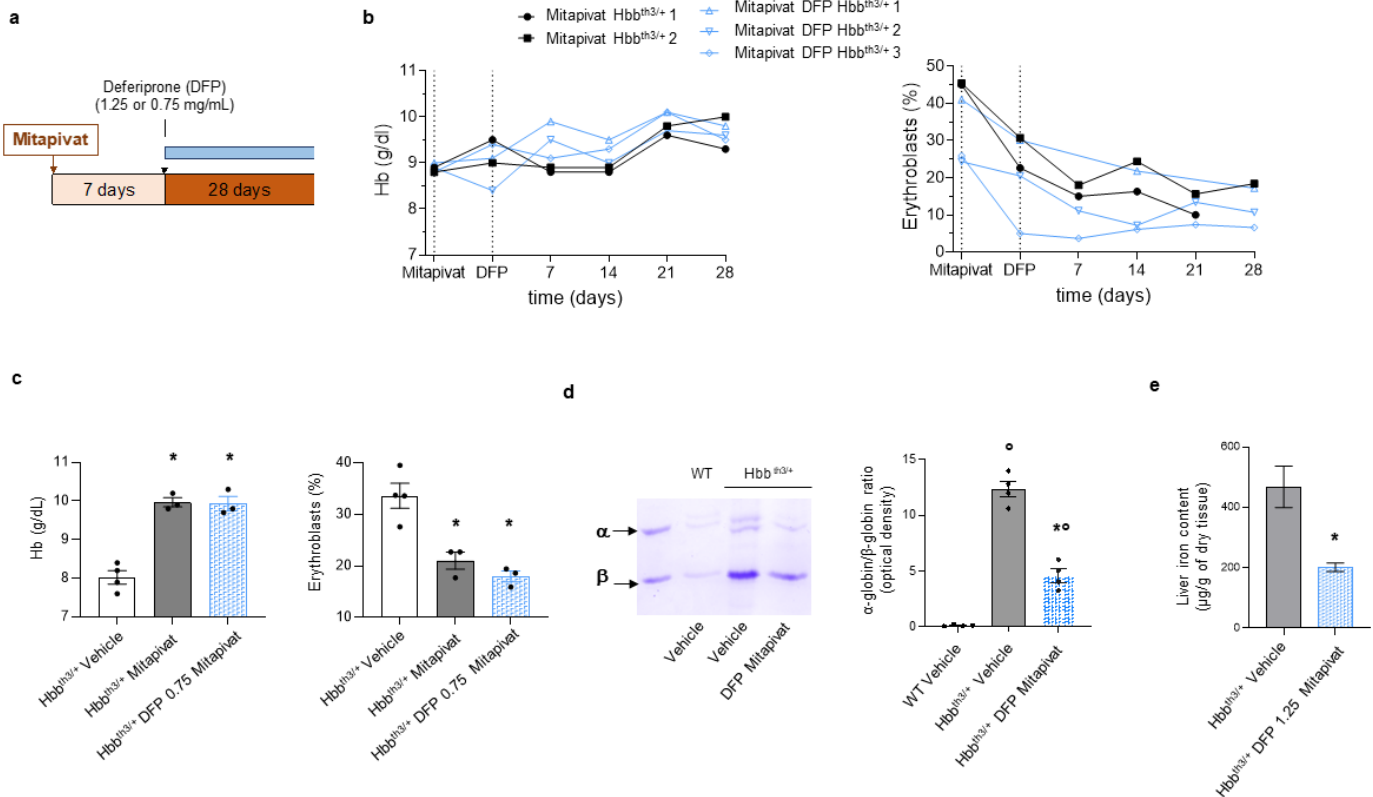
**Figure 1S. a.** Spleen weight to mouse weight ratio in Hbb<sup>th3/+</sup> mice treated with vehicle or exposed to chronic transfusion with or without mitapivat. Data are mean ± SEM ( $n=3-4$ ). \* $P < 0.05$  compared with vehicle Hbb<sup>th3/+</sup> mice and \* $P < 0.05$  compared with vehicle-treated transfused Hbb<sup>th3/+</sup> mice. **b.** Plasma erythropoietin (EPO) levels in Hbb<sup>th3/+</sup> mice treated with vehicle or exposed to chronic transfusion with or without mitapivat. Data are mean ± SEM ( $n=3-4$ ). \* $P < 0.05$  compared with vehicle Hbb<sup>th3/+</sup> mice. **c.** Typical flow cytometric gating strategy used to analyze erythropoietic activity and the maturation index in the bone marrow and in the spleen of Hbb<sup>th3/+</sup> mice exposed to chronic transfusion with or without mitapivat. The following antibodies were used: anti-CD16/CD32 blocking agent, anti-CD44-FITC, CD71-PE, Ter119-APC, CD45 APC-eFluor 780, GR1 APC-Cy7, and CD11b APC-Cy7 (all from eBiosciences, Thermo Fisher Scientific, USA). Analysis was performed with FlowJo software version 10 (BD Biosciences, USA).

Figure 2S



**Figure 2S. a.** Cytofluorimetric quantification strategy of M1 (CD80) and M2 (CD206) expression on spleen M $\Phi$  cell surface from wild-type (WT) or  $Hbb^{th3/+}$  mice exposed to either vehicle or to chronic transfusion with and without mitapivat treatment. Data are mean  $\pm$  SEM (n=3-4). MFI, mean fluorescence intensity. **b.** Plasma creatinine in WT,  $Hbb^{th3/+}$  mice with or without mitapivat,  $Hbb^{th3/+}$  exposed to transfusion with or without mitapivat. Data are mean  $\pm$  SEM (n=3-4). **c.** Real time PCR analysis of *let-7b* and *-7d* relative expression (using the  $\Delta Ct$  method following normalization of cDNA input using RNU-6) in kidneys from WT or  $Hbb^{th3/+}$  mice exposed to either vehicle or to chronic transfusion with and without mitapivat treatment determined with real time PCR. Data are mean  $\pm$  SEM (n=3-4). \*  $P < 0.01$ .

**Figure 3S**



**Figure 3S. a.** Experimental study design to assess the effects of mitapivat on hematologic phenotype of  $\beta$ -thal mice treated DFP, an oral iron chelator. **b.** Hemoglobin (Hb, left panel) and circulating erythroblasts (right panel) in  $Hbb^{th3/+}$  mice treated with mitapivat or mitapivat plus DFP (1.25 mg/mL). Data are shown as single animals (mitapivat  $Hbb^{th3/+}$  n=2; mitapivat plus DFP n=4). **c.** Hemoglobin (Hb, left panel) and circulating erythroblasts (right panel) in  $Hbb^{th3/+}$  mice treated with mitapivat or mitapivat plus DFP (0.75 mg/mL). \* $P < 0.05$  compared with vehicle  $Hbb^{th3/+}$  mice. **d.** Triton acid-urea gel electrophoresis (left panel) of red cell membrane from WT and  $Hbb^{th3/+}$  mice treated with vehicle or mitapivat plus DFP. Arrows show  $\alpha$ -globin and  $\beta$ -globin associated with red cell membrane. Right panel: Gel quantification expressed as  $\alpha$ -globin to  $\beta$ -globin ratio to hemoglobin. Data are mean  $\pm$  SEM (n=4); \* $P < 0.05$  compared with vehicle  $Hbb^{th3/+}$  mice;  $^{\circ}P < 0.05$  compared to WT. **e.** Liver iron concentration (LIC) in  $Hbb^{th3/+}$  mice treated with either vehicle or DFP 1.25 mg/mL plus mitapivat. Data are mean  $\pm$  SEM (n=4-3). \* $P < 0.05$  compared with vehicle  $Hbb^{th3/+}$  mice.